IPPI
Polyolefins Journal, Vol. 6, No. 1 (2019)
DOI: 10.22063/poj.2018.2264.1120

ORIGINAL PAPER

Embedding neat and carboxylated nanodiamonds into polypropylene membranes to enhance antifouling properties

Shahab Hoseinpour[1,2], Yoones Jafarzadeh[1,2*], Reza Yegani[1,2] , Sepideh Masoumi[2]

[1] Faculty of Chemical Engineering, Sahand University of Technology, Tabriz, Iran
[2] Membrane Technology Research Center, Sahand University of Technology, Tabriz, Iran

Received: 30 July 2018, Accepted 19 October 2018

ABSTRACT

The aim of the present work is to enhance the antifouling properties of polypropylene (PP) membrane based on hydrophilicity improvement. Different contents of neat and modified nanodiamond (0.25, 0.50, 0.75 and 1.00 wt.%) were embedded into PP membranes. Nanodiamond nanoparticles were carboxylated by heat treatment method and the presence of carboxyl functional groups on the surface of nanoparticles was confirmed by FTIR analysis. Membranes were then characterized by FESEM, contact angle and tensile strength tests. At the same content of nanoparticles, hydrophilicity, pure water flux and tensile strength of PP/ND-COOH membranes were more than those of PP/ND membranes. Membranes embedded with 0.75 wt. % of neat and modified nanoparticles were used in a submerged membrane bioreactor (SMBR) system along with neat PP membrane. The results showed that critical flux values for neat PP, PP/ND and PP/ND-COOH membranes were 7, 18 and 22 L/(m^2.h), respectively. Analysis of fouling mechanisms revealed that antifouling properties of 0.75 wt. % PP/ND-COOH membrane were higher than those of other two ones so that irreversible fouling ratio decreased from 88.9% for neat PP to 47.8% for PP/ND-COOH membrane. **Polyolefins J (2019) 6: 63-74**

Keywords: Polypropylene, nanodiamond, membrane, MBR, fouling.

INTRODUCTION

Water scarcity remains a big challenge worldwide due to the population growth and therefore, attracts considerable attention toward wastewater reclamation and water reuse [1-3]. Among the wide range of wastewater treatment technologies and water recycling processes, membrane bioreactors (MBRs) have gained an important place in promising wastewater treatment technology [2, 4]. The advantage of using MBR technology for wastewater treatment comprises less hydraulic retention time, less area requirement, high metabolic activity, small footprint demand and low surplus sludge production due to high biomass concentration in the bioreactor and a higher quality of effluent. However, widespread application of MBR process is constrained by membrane fouling which causes severe flux decline, reduces membrane efficiency, and increases operation-

* Corresponding Author - E-mail: yjafarzadeh@sut.ac.ir

al costs due to the increase in energy requirements and the frequency of membrane cleaning and/or replacement [2, 4, 5]. Therefore, suitable material selection for membrane matrix is a key factor in MBR technology.

Polymer membranes are widely used in water and wastewater treatment processes and the most famous are cellulose acetate (CA) [6], polyethylene (PE) [7], polyethersulfone (PES) [8], polyvinylidene fluoride (PVDF) [9], polysulfone (PSF) [8], polyacrylonitrile (PAN) [10], polyether imide (PEI) [11], polyvinyl chloride (PVC) [12] and polypropylene (PP) [13]. Low cast polypropylene has been used extensively as microporous membrane and exhibits good mechanical properties, excellent thermal stability, super chemical resistance, wide applicability and high versatility [14, 15]. PP membrane is prepared via thermally-induced phase separation (TIPS) method and therefore, it is symmetric and microporous in structure and suitable for microfiltration process. Moreover, its life time is more than other conventional membranes like PVDF and PSf due to its chemical stability. Nevertheless, poor hydrophilicity, lack of reactive sites and low surface energy play the role of barrier to its widespread application. Hydrophobic nature of PP leads to adsorption of protein and water contaminants onto membrane surface that results in pore blockage, water flux decline, fouling during the operation, low efficient separation and short lifetime [16, 17].

Many methods have been used to modify polymer membranes and enhance their hydrophilicity including blending with hydrophilic nanoparticles [7], blending with hydrophilic polymers [18], functionalization [19], grafting with hydrophilic polymers [20] and plasma treatment of membrane surface [17]. Among these approaches, blending with hydrophilic nanoparticles is considered as an effective and convenient approach due to its advantages [21-23]. Many studies have been attempted to change the membrane porous structure and enhance the hydrophilicity of polymer membranes by adding inorganic nanoparticles such as Al_2O_3 [24, 25], SiO_2 [26, 27], TiO_2 [28, 29], ZrO_2 [30], Fe_3O_4 [31], CNT [32], GO [33], ZnO [34] and ND [2]. Taghaddosi et al. [16] investigated the effect of nanoclays on the properties and performance of PP membranes. Significant improvement in membranes' hydrophilicity, porosity, pure water flux, flux recovery and rejection has been observed. In addition, tensile strength and thermal stability of the membranes were improved by increasing the content of nanoclays.

Carbon nanomaterials (fullerenes, carbon nanotubes, nanodiamond, and graphene) are among the most important building blocks in modern nanoscience and nanotechnology [35]. Nanodiamond has attracted lots of attention in preparation of composite materials due to its superior mechanical strength, large accessible surface area, thermal conductivity, unique electrical and optical properties, low toxicity, crystallinity, chemical stability, non-porosity, wide band gap, narrow particle size distribution (typically of 4–6 nm), and the possibility of varying the particle properties by means of chemical functionalization of its surface [36-40]. Despite these remarkable features, NDs tend to agglomerate due to Van der Waals forces and electrostatic interactions [36]. To avoid agglomeration, ND would be functionalized via different methods such as fluorination, silanization or carboxylation. NDs functionalized via thermal treatment to produce carboxylated NDs have uniform dispersion and excellent interaction with polymer matrix. The carboxyl groups that remain at the surface of the nanoparticles not only improve the membrane hydrophilicity but also enhance catalytic properties [36, 41]. Several studies have been investigated in incorporation of NDs into polymer membranes. Etemadi et al. [2] studied the effect of detonation nanodiamond (DND) and carboxylated DND (DND-COOH) on the mechanical, thermal and antibacterial properties of CA membrane. The results showed the CA/DND-COOH nanocomposite membrane had the highest values in mechanical, thermal and antibacterial properties in comparison to CA/DND nanocomposite membrane due to the better dispersion of DND-COOH particle compared to DND particle in the CA matrix.

To the best of our knowledge, there is no report about polypropylene/nanodiamond nanocomposite membranes in the literature and therefore, the aim of the present work is to study the effect of neat and functionalized ND on the structure, properties and antifouling behavior of PP membranes. In order to achieve an effective dispersion of ND nanoparticles in PP membrane matrix, ND nanoparticles should be

functionalized before embedding into polymer matrix. Moreover, it has been accepted that the surface energy and the polarity of the PP membrane increase significantly at the presence of maleic anhydride-grafted polypropylene (PP-g-MA) [16, 42, 43]. ND nanoparticles were carboxylated thermally, and PP-g-MA was also used to enhance the compatibility between ND and PP. The membranes were then characterized and used in the MBR system with pharmaceutical feed.

EXPERIMENTAL

Materials

Commercial grade of isotactic PP (iPP, EPD60R, MFI= 0.35 g/10 min) was supplied from Arak Petrochemical Company. PP-g-MA (2% MA) was purchased by Pluss Polymer (India). Paraffin as diluent and acetone as extractant were purchased from Atlas Shimi and Merck, respectively. ND nanoparticles were procured from Nabond Technology Co., Ltd., China. Adapted activated sludge and influent wastewater were supplied by the wastewater treatment plant of Dana Pharmaceutical Company of Tabriz, Iran.

Carboxylation of ND

Pristine ND was dried at 80°C for 2 h in a vacuum dryer and then treated thermally at 430-450°C for 1.5 h. Carboxylated ND was denoted by ND-COOH.

Preparation of membranes

Thermally-induced phase separation (TIPS) method was applied to prepare membranes. Different amounts of ND or COOH-ND (0.25, 0.50, 0.75 and 1 wt. % polymer) were dispersed into 50 g paraffin by using sonication by probe system (Sonopuls HD 3200, Bandelin) for 2 h. Then, 16.17 g PP and 0.5 g PP-g-MA were added to the suspension and melt blended at 170°C for 2 h. The solution was then allowed to degas for 30 min and cast on a preheated glass by using a doctor blade. The plate was immediately quenched in the water bath of 27-30°C to induce phase separation. Then, the membranes were immersed into acetone to extract the diluent. Finally, membranes were dried at room temperature for 24 h. For preparation of neat PP membrane, paraffin and PP were melt blended at 170°C for 2 h. The other procedure was the same to the nanocomposite membranes preparation.

Characterization

The FT-IR spectra of pristine and carboxylated ND nanoparticles were taken on Tensor 27 FTIR spectrometer. The morphology of the membranes was studied by a field emission scanning electron microscope (FESEM; MIRA3 FEG-SEM, Tescan). Samples were fractured in liquid nitrogen and coated with gold by sputtering before observation. Hydrophilic/hydrophobic characteristics of the membranes were examined by measuring the contact angle between membrane surface and water droplet using a contact angle goniometer (PGX, Thwing-Albert Instrument Co.). In order to minimize the experimental error, the average of five measurements was reported. Tensile strength of membranes were measured using a tensile test machine (STM-5, SANTAM, Iran). The samples were cut into 5 cm × 1cm in length and width, respectively. For each membrane, three samples were tested at an extension rate of 50 mm/min at room temperature and the average values were reported. Pure water flux (PWF) of membranes was determined as follows: membrane module was submerged in water bath and connected to a vacuum pump to provide transmembrane pressure of 0.7 bar. PWF was calculated using the following equation:

$$J_0 = \frac{M}{A \cdot t} \quad (1)$$

Where J_0 is PWF, M is collected mass of water, A is the area of membrane and t is the time.

MBR run

In this study, three membranes including neat PP, 0.75 wt. % PP/ND and 0.75 wt. % PP/ND-COOH membranes were selected to be used in a lab-scale submerged MBR apparatus with 12 L effective volume. An air diffuser under the membrane module provided continuous aeration to maintain the dissolved oxygen for microorganisms at desired levels and also to provide a shear force to hinder deposition of activated sludge on the membrane surface. The membrane module was connected to a vacuum pump to provide transmembrane pressure. Influent wastewater and adapted

activated sludge were supplied by the wastewater treatment plant of Dana Pharmaceutical Company of Tabriz, Iran. The chemical oxygen demand (COD) of feed wastewater stream was about 2800 mg/L. The MBR operated at the solids retention time (SRT) of 35 days and a hydraulic retention time (HRT) of 24 h. Mixed liquor suspended solid's (MLSS) concentration was measured daily and was kept about 7500-8000 mg/L. The critical transmembrane pressure (TMP) was measured for all membranes by the TMP-step following a method described elsewhere [24].

Fouling analysis

After about 360 min MBR run, membrane module was removed from the MBR and submerged in the water bath to evaluate water flux of membrane after fouling (J1). Afterward, the biofilm on the membrane surface was removed by a tissue and the membrane was backwashed by DI water. Subsequently, the pure water flux after cleaning (J2) was measured. Fouling properties of the membrane were calculated as follows:

$$TFR = \frac{J_0 - J_1}{J_0} \quad (2)$$

$$RFR = \frac{J_2 - J_1}{J_0} \quad (3)$$

$$IFR = \frac{J_0 - J_2}{J_0} \quad (4)$$

$$FR = \frac{J_2}{J_0} \quad (5)$$

where TFR, RFR, IFR and FR are total fouling ratio, reversible fouling ratio, irreversible fouling ratio and flux recovery, respectively. COD removal was estimated by measuring COD_s of effluent (COD_E) and influent (COD_I) based on absorbance method as described elsewhere [34] and using the following equation:

$$\text{COD Removal (\%)} = (1 - \frac{COD_E}{COD_I}) \times 100 \quad (6)$$

RESULTS AND DISCUSSION

Characterization of carboxylated ND

FTIR was employed to explore the introduced functional groups onto the surface of treated NDs. The spectra of ND and ND-COOH nanoparticles are shown in Figure 1. For ND NPs, the absorption peaks at 2858.4 and 2926.9 cm^{-1} correspond to the asymmetric and symmetric stretching vibration of C-H band, respectively, and can be related to CH, CH_2, CH_3. Also, the absorption bands at 1331.2 cm-1 can be attributed to the deformation vibration of C-H band in alkyl group. Presence of hydroxyl group; -OH, and deformation vibrations of O-H band on pristine ND can be revealed by absorption peaks at 1626.9 cm^{-1} and 3450.5 cm^{-1}. The peaks at 1733.9 cm^{-1} and 1131.2 cm^{-1} are attributed to the presence of oxygen containing functional groups which are attributed to the stretching vibration of carbonyl, C=O and ether, C-O-C groups, respectively [44]. Comparison of the FTIR spectra of neat and carboxyated ND particles in Figure 1 reveals that the variety of surface functional groups in raw DND has been converted into their oxidized derivatives. After treatment of NDs, the peaks at 2858.4 cm^{-1} and 2926.9 cm^{-1} that correspond to the C-H groups were completely disappeared. By conversion of some oxygen containing groups like ketone, alcohol and ester to carboxylic group, the absorption peak of C-O is shifted from 1733.9 cm^{-1} to 1793.6 cm^{-1} [45].

Contact angle

The contact angle is an important parameter for measuring surface hydrophilicity [46]. The smaller contact angle leads to higher hydrophilicity [47]. The static contact angle between water drop and surfaces of the PP and nanocomposite membranes was measured and the data are illustrated in Figure 2. It can be seen that the contact angle of both nanocomposite membranes decreased considerably compared with

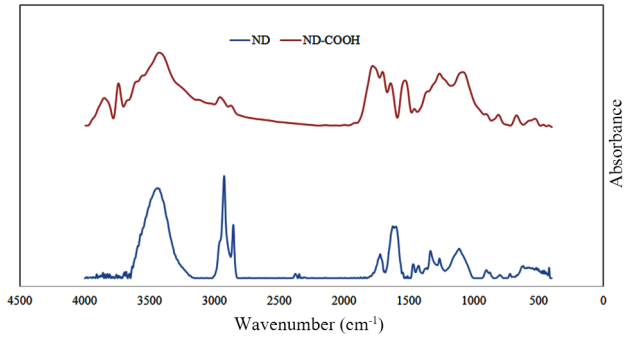

Figure 1. FTIR spectra of pristine ND and ND-COOH nanoparticles.

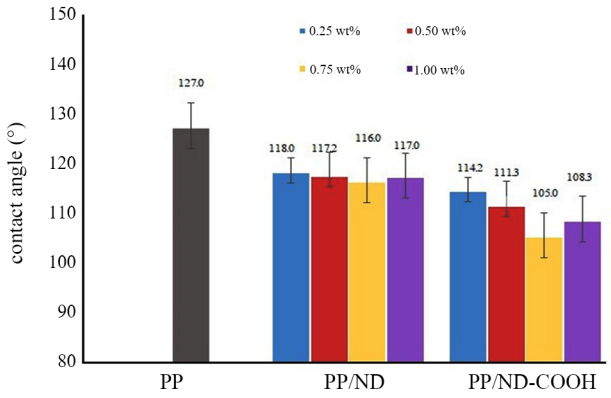

Figure 2. Contact angle measurements for PP, PP/ND and PP/COOH-ND membranes.

neat PP membrane. This indicates that the hydrophilicity of the membranes increased as a result of embedding pristine and carboxylated ND. In addition, at the same contents of nanoparticles, the COOH-ND embedded membranes exhibited lower contact angles in comparison to ND/PP membranes due to the presence of abundant hydrophilic groups on the COOH-ND nanoparticles. For example, contact angle decreased from 127.0° for neat PP membrane to 116.0° and 105.0° for 0.75 wt. % PP/ND and PP/COOH-ND membranes, respectively. However, when the content of NDs and COOH-NDs increased to 1.0 wt. %, the contact angle value increased which it could be attributed to the agglomeration of nanoparticles, which consequently resulted in non-uniform dispersion of nanoparticles [48]. In general, increasing the hydrophilicity of the membrane improves fouling resistance as well as water permeability because water adsorption of hydrophilic membranes is higher than that of hydrophobic ones [49, 50].

Morphology

Cross section and surface FESEM images of neat PP and 0.75 wt. % of ND and ND-COOH membranes are shown in Figure 3. More and smaller pores can be seen in the PP/ND and PP/ND-COOH membranes due to the presence of ND particles. In fact, by addition

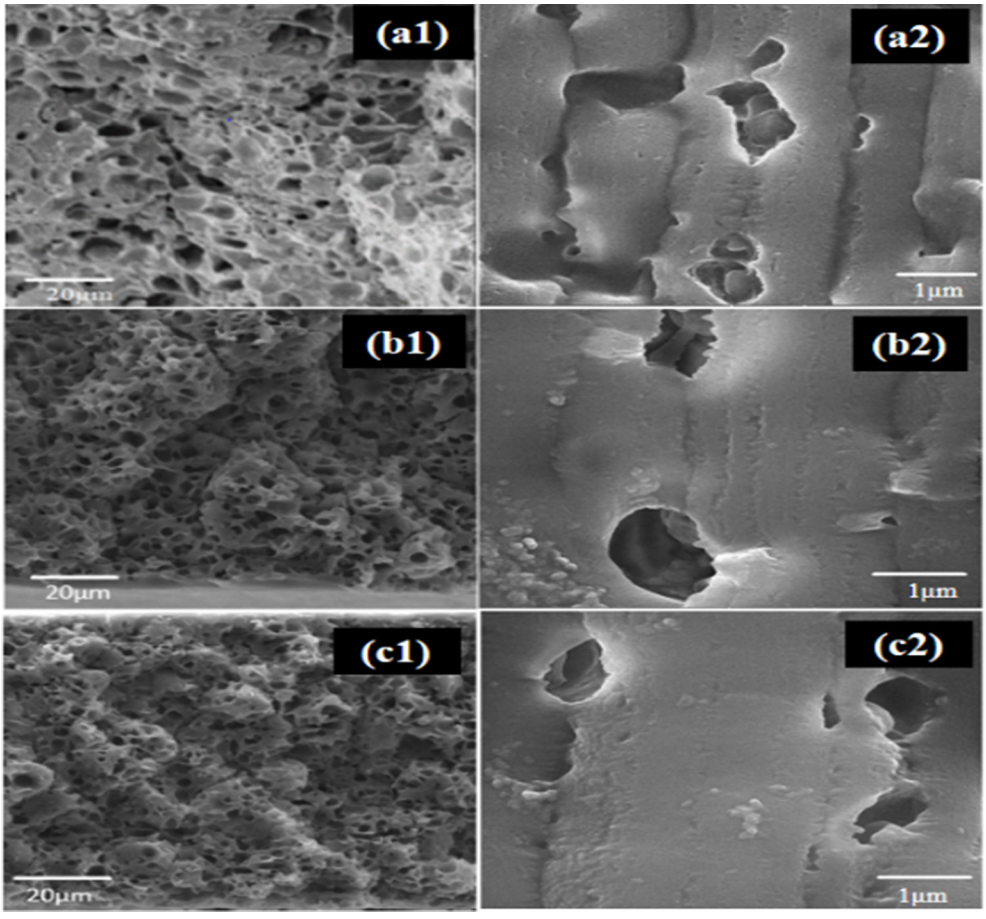

Figure 3. Cross section (left) and surface (right) FESEM images of three prepared membranes. (a) neat PP, (b) PP/ND 0.75 wt.% (c) PP/ND-COOH 0.75 wt.%.

of ND and ND-COOH particles to dope solution, the cooling rate increased during quench step because the thermal conductivity of solutions containing nanodiamond particles are higher than that of PP solution. It is well known that higher cooling rate leads to the smaller pores in thermally-induced phase separation [51, 52]. Moreover, comparing Figures 3b and 3c reveals that PP/ND-COOH membrane has further and smaller pores which can be explained by proper distribution of nanoparticles in the membrane matrix. Figure 3 also shows the agglomeration of neat ND nanoparticles in the PP/ND membrane and it can be seen that the modification of ND prevents the agglomeration of nanoparticles.

Mechanical properties

It is generally accepted that the addition of inorganic nanoparticles into the polymeric matrix changes the polymer's mechanical properties [53]. The impact of ND and COOH-ND presence and concentrations on the tensile strength of prepared membranes are presented in Figure 4. For neat PP membrane, the tensile strength was 3.70 MPa and by increasing the content of both ND and COOH-ND up to 0.5 wt. % the tensile strength of nanocomposite membranes increased up to 4.61 and 5.26 MPa, respectively. The increase in tensile strength can be attributed to excellent mechanical properties of ND. It is obvious that the increase in tensile strength of COOH-ND embedded PP membranes is more pronounced than ND embedded PP membranes. This can be explained by NDs treatment which reduces the tendency of ND particles to agglomerate. However, further increase in ND and COOH-ND content decreased tensile strength due to the aggregation of particles. It should be noted that at the same content of nanoparticles, tensile strength of PP/COOH-ND membranes are more than that of PP/ND ones even at higher contents of nanoparticles, indicating that carboxylation of ND nanoparticles reduces ND agglomeration in polymer matrix. These results are similar to the results reported elsewhere [54, 55].

Pure water flux

The pure water flux values of all fabricated membranes are illustrated in Figure 5. Compared with the pure water flux of the pristine PP membrane (14.30 L/m^2.h), the pure water flux of PP/ND and PP/COOH-ND nanocomposite membranes were enhanced significantly by addition of nanoparticles up to 0.75 wt.%. When the content of ND and COOH-ND increased to 0.75 wt. %, the water flux of PP/ND and PP/COOH-ND membranes reached a maximum value of 99.96 kg/(m^2.h) and 183.88 kg/(m^2.h), respectively. In general, the hydrophilicity and morphology of a membrane impact its pure water flux. At the presence of the nanoparticles in casting solution, the interaction between polymer chains and the nanoparticles may disrupt the polymer chain packing and therefore, improves water permeability due to the introduction of free volumes between the polymer chains and nanofiller interface [58]. Figure 4 shows that the porosity of PP/ND and PP/COOH-ND membranes was higher than that of neat PP membrane. In addition, the contact angle of membranes decreased with increasing nanoparticles content as shown in Figure, which can enhance water permeability throughout the membranes. Comparing the results indicates that the PP/

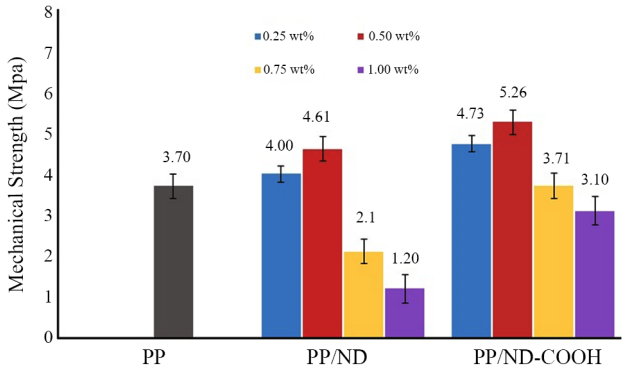

Figure 4. Tensile strength content values for prepared membranes.

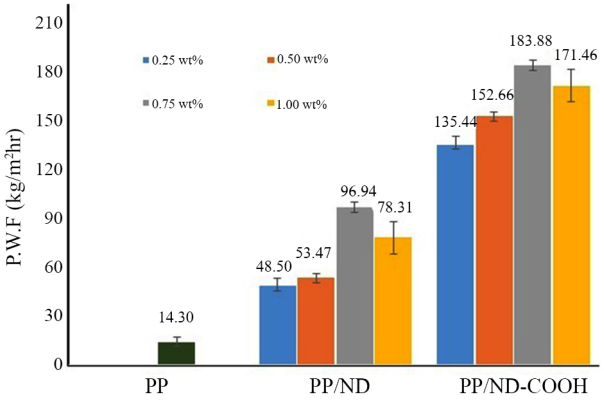

Figure 5. Pure water flux of the prepared membranes.

COOH-ND nanocomposite membranes had higher pure water flux than the PP/ND which could be explained by the higher hydrophilicity of them. The decrease in PWF of 1.0 wt. % nanocomposite membranes may be due to the agglomeration of nanoparticles [57].

MBR operation and fouling analysis

Three membranes including neat PP, 0.75 wt. % PP/ND and 0.75 wt. % PP/COOH-ND were selected and used in MBR system to investigate the effect of pristine and modified NDs on the performance of PP membrane. Figure 6 shows that the critical flux for neat PP membrane is about 7 L/(m^2.h) and the presence of pristine ND enhanced the critical flux up to 18 L/(m^2.h). Interestingly, the critical flux of PP/COOH-ND membrane reached to 22 L/(m^2.h). These results revealed that the incorporation of ND and COOH-ND nanoparticles into PP membranes increased the critical flux which significantly affects membrane fouling

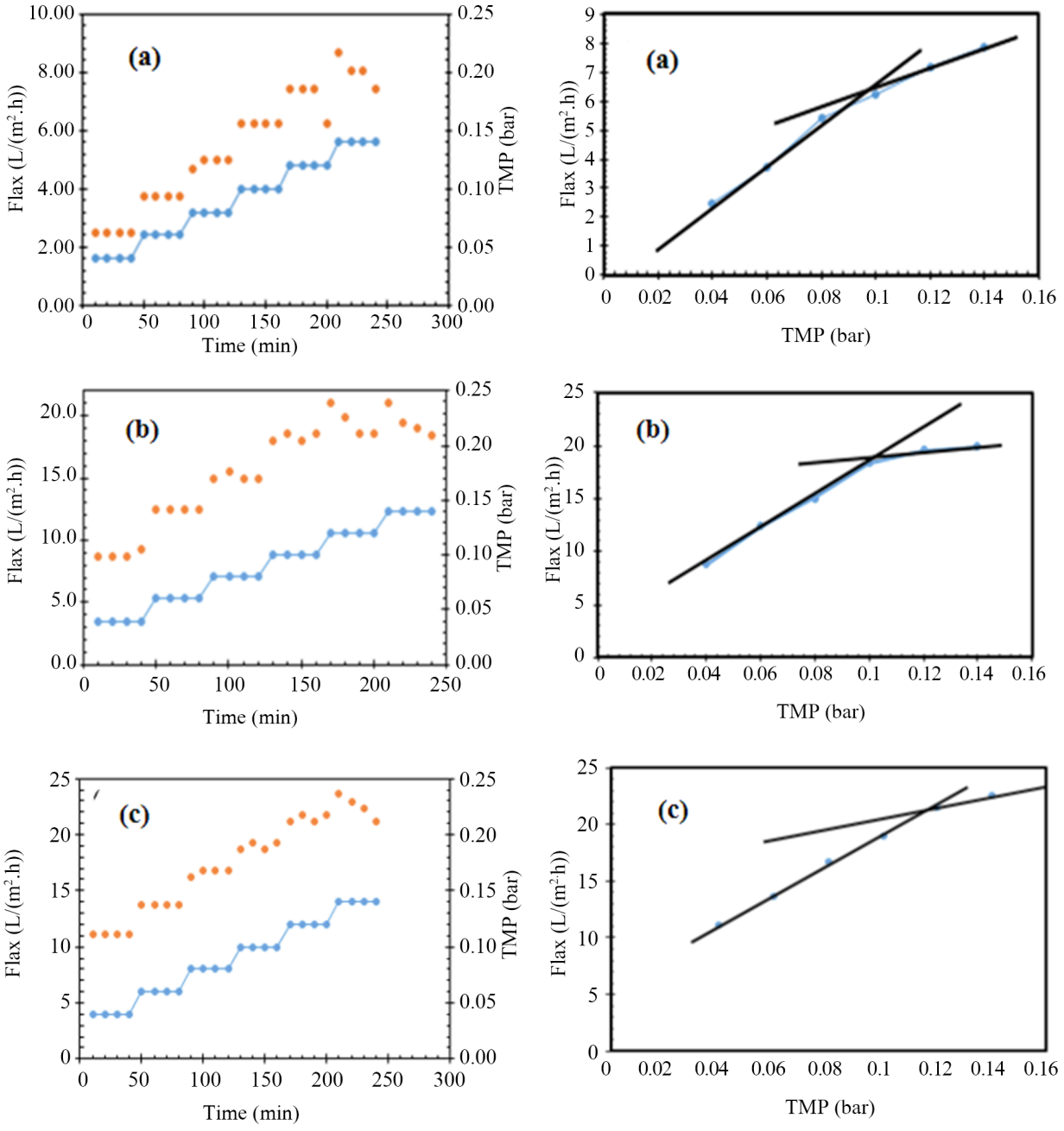

Figure 6. Determination of the critical flux for (a) PP, (b) PP/ND (0.75 wt.%) and (c) PP/ND-COOH (0.75 wt.%) membranes.

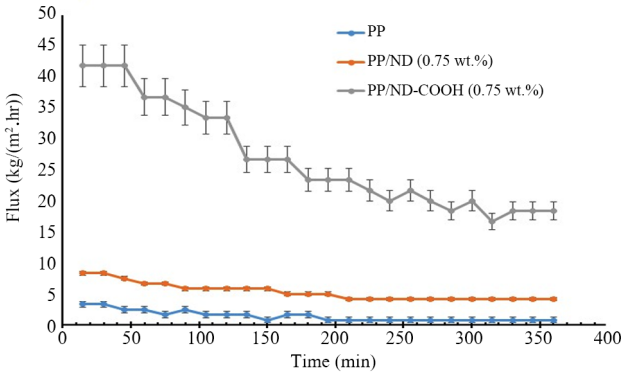

Figure 7. Flux of PP, PP/ND and PP/COOH-ND membranes.

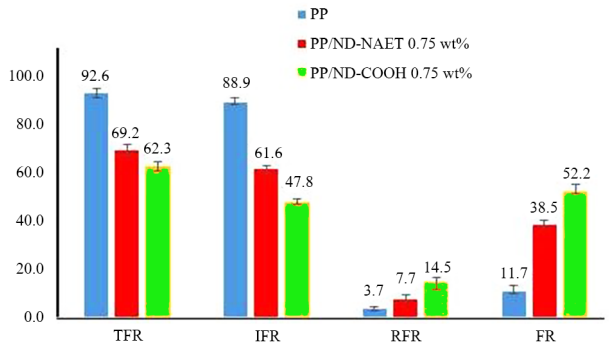

Figure 8. Fouling parameters of neat PP, PP/ND and PP/ND-COOH membranes.

during MBR operation.

The results of filtration during MBR operation running at subcritical pressure of 0.1 bar for three membranes are shown in Figure 7. It can be seen that both PP/ND and PP/COOH-ND membranes exhibited higher flux than the neat PP membrane. For neat PP membrane, flux started from 3.41 kg/(m^2.h) and declined to 0.57 kg/(m^2.h) after 360 min which means that neat PP membrane preserved about 17% of its initial flux after 360 min. For 0.75 wt. % PP/ND membrane, however, the initial and final flux values were 9.05 and 4.91 kg/(m^2.h), respectively, indicating that antifouling ability of PP/ND membrane increased due to the presence of ND nanoparticles. On the other hand, the flux of 0.75 wt. % PP/COOH-ND membrane decreased from 41.16 to 20.93 kg/m^{2}h meaning that the decline is about 50%. These results show that the presence of neat and modified NDs enhanced antifouling properties of PP membrane and modification of ND nanoparticles had better antifouling effect than pristine NDs. This can be related to the hydrophilicity and antibacterial properties of the nanoparticles which reduce adsorption of hydrophobic foulants on membrane's surface.

Fouling analysis of membranes was carried out by calculating the fouling parameters including RFR, IFR, TFR, and FR and the results are shown in Figure 8. The results indicate that TFR value for neat PP membrane was the highest (92.6%) and it decreased to 69.2 and 62.3 % for PP/ND and PP/COOH-ND membranes, respectively. In addition, IFR for the last membrane is 47.8% whereas the IFR values of PP/ND and neat PP membranes are 61.6 and 88.9, respectively. These results show that even though antifouling properties of PP/ND membrane is better than that of neat PP membrane, but carboxylation of ND nanoparticles resulted in membrane with more antifouling properties. The improved antifouling properties of PP/COOH-ND membrane can be ascribed to the hydrophilicity and antibacterial effect of COOH-ND which prevent the foulants from attaching to membrane surface. Water molecules tend to attach to hydrophilic surfaces and form a water layer on membrane surface which prevent foulants from approaching the surface [58]. Therefore, higher hydrophilicity of the PP/ND-COOH membranes results in a lower fouling tendency than those of the PP and PP/ND membranes.

Table 1 shows a comparison between the results of the present work with other industrial membranes such as PVDF and cellulose acetate. It can be seen that PP/ND-COOH membranes would be applied extensively in MBR systems for wastewater treatment.

Table 1. Comparison of PP/ND-COOH membrane in this work with other membranes used in MBR systems.

Membrane	Results	Reference
PVDF/GO-CNC	Higher wettability and permeability, lower protein adsorption, higher flux recovery ratio and lower irreversible fouling.	[59]
PVDF/GO	Sustained permeability, lower cleaning frequency, fewer EPS adsorption.	[60]
MWCNTs/PES	Higher permeability, hydrophilicity and antifouling properties.	[4]
PEG-ND/CA	Higher critical flux, higher antifouling and, lower adsorption of proteins.	[2]
PP/ND-COOH	Higher hydrophilicity and water flux, higher critical flux, higher antifouling properties.	Present work

CONCLUSION

Pristine and carboxylated nanodiamond were embedded into polypropylene membranes. ND nanoparticles were carboxylated by heat treatment method and the presence of carboxyl functional groups on the surface of nanoparticles was confirmed by FTIR analysis. The results showed that at the same content of pristine and carboxylated ND nanoparticles, hydrophilicity, pure water flux and tensile strength of PP/ND-COOH membranes were more than those of PP/ND membranes. Membranes embedded with 0.75 wt. % of neat and modified nanoparticles were used in a submerged membrane bioreactor (SMBR) system along with neat PP membrane. The results showed that critical flux values for neat PP, PP/ND and PP/ND-COOH membranes were 7, 18 and 22 L/(m^2.h), respectively. Analysis of fouling mechanisms revealed that antifouling properties of 0.75 wt. % PP/ND-COOH membrane were higher than those of other two ones so that irreversible fouling ratio decreased from 88.9% for neat PP to 47.8% for PP/ND-COOH membrane. The improved antifouling properties of PP/COOH-ND membrane were attributed to the hydrophilicity and antibacterial effect of carboxyl groups on the ND nanoparticles which prevent the foulants from attaching to membrane surface.

REFERENCES

1. Molinos-Senante M, Donoso G (2016) Water scarcity and affordability in urban water pricing: A case study of Chile. Utilities Policy 43: 107-116
2. Etemadi H, Yegani R, Seyfollahi M (2017) The effect of amino functionalized and polyethylene glycol grafted nanodiamond on anti-biofouling properties of cellulose acetate membrane in membrane bioreactor systems. Separ Purif Technol 177: 350-362
3. Liu J, Liu Q, Yang H (2016) Assessing water scarcity by simultaneously considering environmental flow requirements, water quantity, and water quality. Ecol Indic 60: 434-441
4. Rahimi Z, Zinatizadeh A, Zinadini S (2015) Preparation of high antibiofouling amino functionalized MWCNTs/PES nanocomposite ultrafiltration membrane for application in membrane bioreactor. J Ind Eng Chem 29: 366-374
5. Maqbool T, Khan SJ, Lee C-H (2014) Effects of filtration modes on membrane fouling behavior and treatment in submerged membrane bioreactor. Bioresour Technol 172: 391-395
6. Abedini R, Mousavi SM, Aminzadeh R (2011) A novel cellulose acetate (CA) membrane using TiO_2 nanoparticles: preparation, characterization and permeation study. Desalination 277: 40-45
7. Jafarzadeh Y, Yegani R, Tantekin-Ersolmaz S (2015) Effect of TiO_2 nanoparticles on structure and properties of high density polyethylene membranes prepared by thermally induced phase separation method. Polym Adv Technol 26: 392-398
8. Daraei P, Madaeni SS, Ghaemi N, Monfared HA, Khadivi MA (2013) Fabrication of PES nanofiltration membrane by simultaneous use of multi-walled carbon nanotube and surface graft polymerization method: comparison of MWCNT and PAA modified MWCNT. Separ Purif Technol 104: 32-44
9. Li Z-K, Lang W-Z, Miao W, Yan X, Guo Y-J (2016) Preparation and properties of PVDF/SiO_2 @ GO nanohybrid membranes via thermally induced phase separation method. J Membrane Sci 511: 151-161
10. Kim I-C, Yun H-G, Lee K-H (2002) Preparation of asymmetric polyacrylonitrile membrane with small pore size by phase inversion and post-treatment process. J Membrane Sci 199: 75-84
11. Nunes S, Peinemann K, Ohlrogge K, Alpers A, Keller M, Pires A (1999) Membranes of poly (ether imide) and nanodispersed silica, Journal of Membrane Science 157: 219-226
12. Behboudi A, Jafarzadeh Y, Yegani R (2016) Preparation and characterization of TiO_2 embedded PVC ultrafiltration membranes, Chem Eng Res Design, 114: 96-107
13. Saffar A, Carreau PJ, Kamal MR, Ajji A (2014) Hydrophilic modification of polypropylene microporous membranes by grafting TiO2

nanoparticles with acrylic acid groups on the surface. Polymer 55: 6069-6075
14. Chen H, Ma W, Xia Y, Gu Y, Cao Z, Liu C, Yang H, Tao S, Geng H, Tao G (2017) Improving amphiphilic polypropylenes by grafting poly (vinylpyrrolidone) and poly (ethylene glycol) methacrylate segments on a polypropylene microporous membrane. Appl Surf Sci 419: 259-268
15. Sathe SN, Rao GS, Devi S (1994) Grafting of maleic anhydride onto polypropylene: Synthesis and characterization. J Appl Polym Sci 53: 239-245
16. Taghaddosi S, AkbariA, Yegani R (2017) Preparation, characterization and anti-fouling properties of nanoclays embedded polypropylene mixed matrix membranes. Chem Eng Res Design 125: 35-45
17. Kang MS, Chun B, Kim SS (2001) Surface modification of polypropylene membrane by low-temperature plasma treatment. J Appl Polym Sci 81: 1555-1566
18. Kumar R, Isloor AM, Ismail A, Rashid SA, Al Ahmed A (2013) Permeation, antifouling and desalination performance of TiO_2 nanotube incorporated PSf/CS blend membranes. Desalination 316: 76-84
19. Chung T, Lee S, (1997) New hydrophilic polypropylene membranes; fabrication and evaluation. J Appl Polym Sci 64: 567-575
20. Ulbricht M, Matuschewski H, Oechel A, Hicke H-G (1996) Photo-induced graft polymerization surface modifications for the preparation of hydrophilic and low-proten-adsorbing ultrafiltration membranes. J Membrane Sci 115: 31-47
21. Jafarzadeh Y, Yegani R, Sedaghat M (2015) Preparation, characterization and fouling analysis of ZnO/polyethylene hybrid membranes for collagen separation. Chem Eng Res Design 94: 417-427
22. Liang S, Xiao K, Mo Y, Huang X (2012) A novel ZnO nanoparticle blended polyvinylidene fluoride membrane for anti-irreversible fouling. J Membrane sci 394: 184-192
23. Balta S, Sotto A, Luis P, Benea L, Van der Bruggen B, Kim J (2012) A new outlook on membrane enhancement with nanoparticles: the alternative of ZnO. J Membrane Sci 389: 155-161
24. Liu F, Abed MM, Li K (2011) Preparation and characterization of poly (vinylidene fluoride) (PVDF) based ultrafiltration membranes using nano γ-Al_2O_3. J Membrane Sci 366: 97-103
25. Yan L, Li YS, Xiang CB (2005) Preparation of poly (vinylidene fluoride)(pvdf) ultrafiltration membrane modified by nano-sized alumina (Al 2O3) and its antifouling research. Polymer 46: 7701-7706
26. Ahsani M, Yegani R (2015) Study on the fouling behavior of silica nanocomposite modified polypropylene membrane in purification of collagen protein. Chem Eng Res Design 102: 261-273
27. Ahmad A, Majid M, Ooi B (2011) Functionalized PSf/SiO_2 nanocomposite membrane for oil-in-water emulsion separation. Desalination 268: 266-269
28. Rahimpour A, Jahanshahi M, Rajaeian B, Rahimnejad M (2011) TiO_2 entrapped nano-composite PVDF/SPES membranes: Preparation, characterization, antifouling and antibacterial properties. Desalination 278: 343-353
29. Yu L-Y, Xu Z-L, Shen H-M, Yang H (2009) Preparation and characterization of PVDF–SiO_2 composite hollow fiber UF membrane by sol–gel method. J Membrane Sci 337: 257-265
30. Bottino A, Capannelli G, Comite A (2002) Preparation and characterization of novel porous PVDF-ZrO_2 composite membranes. Desalination 146: 35-40
31. Gholami A, Moghadassi A, Hosseini S, Shabani S, Gholami F (2014) Preparation and characterization of polyvinyl chloride based nanocomposite nanofiltration-membrane modified by iron oxide nanoparticles for lead removal from water. J Ind Eng Chem 20: 1517-1522
32. Yin J, Zhu G, Deng B (2013) Multi-walled carbon nanotubes (MWNTs)/polysulfone (PSU) mixed matrix hollow fiber membranes for enhanced water treatment. J Membrane Sci 437: 237-248
33. Meng N, Priestley RCE, Zhang Y, Wang H, Zhang X (2016) The effect of reduction degree of GO

nanosheets on microstructure and performance of PVDF/GO hybrid membranes. J Membrane Sci 501: 169-178
34. Shen L, Bian X, Lu X, Shi L, Liu Z, Chen L, Hou Z, Fan K (2012) Preparation and characterization of ZnO/polyethersulfone (PES) hybrid membranes. Desalination 293: 21-29
35. Basiuk EV, Santamaría-Bonfil A, Meza-Laguna V, Gromovoy TY, Alvares-Zauco, E, Contreras-Torres FF, Rizo J, Zavala G, Basiuk VA (2013) Solvent-free covalent functionalization of nanodiamond with amines. Appl Surf Sci 275: 324-334
36. Wahab Z, Foley EA, Pellechia PJ, Anneaux BL, Ploehn HJ (2015) Surface functionalization of nanodiamond with phenylphosphonate. J Colloid Interf Sci 450: 301-309
37. Neitzel I, Mochalin V, Knoke I, Palmese GR, Gogotsi Y (2011) Mechanical properties of epoxy composites with high contents of nanodiamond. Composites Sci Technol 71: 710-716
38. Rakha SA, Ali N, Haleem YA, Alam F, Khurram AA, Munir A (2014) Comparison of mechanical properties of acid and UV ozone treated nanodiamond epoxy nanocomposites. J Mater Sci Technol 30: 753-758
39. Neitzel I, Mochalin V, Niu J, Cuadra J, Kontsos A, Palmese GR , Gogotsi Y (2012) Maximizing Young's modulus of aminated nanodiamond-epoxy composites measured in compression. Polymer 53: 5965-5971
40. Behler KD, Stravato A, Mochalin V, Korneva G, Yushin G, Gogotsi Y (2009) Nanodiamond-polymer composite fibers and coatings. ACS nano 3: 363-369
41. Hajiali F, Shojaei A (2016) Silane functionalization of nanodiamond for polymer nanocomposites-effect of degree of silanization. Colloids Surfaces A: Physicochem Eng Aspects 506: 254-263
42. Oromiehie A, Ebadi-Dehaghani H, Mirbagheri S (2014) Chemical modification of polypropylene by maleic anhydride: Melt grafting, characterization and mechanism. Int J Chem Eng Appl 5: 117
43. Wang P-H Ghoshal S, Gulgunje P, Verghese N, Kumar S (2016) Polypropylene nanocomposites with polymer coated multiwall carbon nanotubes. Polymer 100: 244-258
44. Li C-C, Huang C-L (2010) Preparation of clear colloidal solutions of detonation nanodiamond in organic solvents. Colloids Surfaces A: Physicochem Eng Aspects 353: 52-56
45. Aris A, Shojaei A, Bagheri R (2015) Cure kinetics of nanodiamond-filled epoxy resin: Influence of nanodiamond surface functionality. Ind Eng Chem Res 54: 8954-8962
46. Palacio L, Calvo J, Pradanos P, Hernandez A, Väisänen P, Nyström M (1999) Contact angles and external protein adsorption onto UF membranes. J Membrane Sci 152: 189-201
47. Zhao Y, Xu Z, Shan M, Min C, Zhou B, Li Y, Li B, Liu L, Qian X (2013) Effect of graphite oxide and multi-walled carbon nanotubes on the microstructure and performance of PVDF membranes. Separ Purif Technol 103: 78-83
48. Xu Z, Zhang J, Shan M, Li Y, Li B, Niu J, Zhou B, Qian X (2014) Organosilane-functionalized graphene oxide for enhanced antifouling and mechanical properties of polyvinylidene fluoride ultrafiltration membranes. J Membrane Sci 458: 1-13
49. Yuliwati E, Ismail AF (2011) Effect of additives concentration on the surface properties and performance of PVDF ultrafiltration membranes for refinery produced wastewater treatment. Desalination 273: 226-234
50. Khalid A, Al-Juhani AA, Al-Hamouz OC, Laoui T, Khan Z, Atieh MA (2015) Preparation and properties of nanocomposite polysulfone/multi-walled carbon nanotubes membranes for desalination. Desalination 367: 134-144
51. Matsuyama H, Yuasa M, Kitamura Y, Teramoto M, Lloyd DR (2000) Structure control of anisotropic and asymmetric polypropylene membrane prepared by thermally induced phase separation. J Membrane Sci 179: 91-100
52. Branson BT, Beauchamp PS, Beam JC, Lukehart CM, Davidson JL (2013) Nanodiamond nanofluids for enhanced thermal conductivity. Acs Nano 7: 3183-3189
53. Nguyen VG, Thai H, Mai DH, Tran HT, Vu MT (2013) Effect of titanium dioxide on the properties of polyethylene/TiO_2 nanocomposites.

Composites B: Eng 45: 1192-1198
54. Etemadi H, Yegani R, Babaeipour V (2017) Performance evaluation and antifouling analyses of cellulose acetate/nanodiamond nanocomposite membranes in water treatment. J Appl Polym Sci 134: 44873
55. Wu T, Farnood R, O'Kelly K, Chen B (2014) Mechanical behavior of transparent nanofibrillar cellulose–chitosan nanocomposite films in dry and wet conditions. J Mech Behav Biomed Mater 32: 279-286
56. Wang W-Y, Shi J-Y, Wang J-L, Li Y-L, Gao N-N, Liu Z-X, Lian W-T (2015) Preparation and characterization of PEG-g-MWCNTs/PSf nano-hybrid membranes with hydrophilicity and antifouling properties. RSC Adv 5: 84746-84753
57. Zhao S, Wang P, Wang C, Sun X, Zhang L (2012) Thermostable PPESK/TiO_2 nanocomposite ultrafiltration membrane for high temperature condensed water treatment. Desalination 299: 35-43
58. Arthanareeswaran G, Devi TS, Raajenthiren M (2008) Effect of silica particles on cellulose acetate blend ultrafiltration membranes: Part I. Separ Purif Technol 64: 38-47
59. Lv J, Zhang G, Zhang H, Yang F (2018) Graphene oxide-cellulose nanocrystal (GO-CNC) composite functionalized PVDF membrane with improved antifouling perfornabce in MBR: Behaviour and mechanism. Chem Eng J 352: 765-773
60. Zhao C, Xu X, Chen J, Wang G, Yang F (2014) Highly effective antifouling performance of PVDF/graphene oxide composite membrane in membrane biorector (MBR) system. Desalination 340: 59-66